CHAPTER-3: DESIGN AND IMPLEMENTATION OF FRAMEWORK FOR THE RESTORATION AND ENHANCEMENT OF CAPSULE ENDOSCOPY IMAGES

In this chapter, we have designed and implemented a framework for the restoration of CE images using partial differential equations based filter. This chapter includes types of noises to which a CE image is exposed, mechanism of removal of noisy components and retaining of important lost components in a controlled mechanism so that the quality of the image is maintained while the noise is removed.

3.1 Introduction

CE images exhibit random noise, motion blur, and illumination related degradations. These degradations reduce the efficiency of the CAD system. The proposed restoration process aims to minimize degradations as much as possible.

In the CE procedure, the limitations in the image quality and the frame rate are inherent due to the problem of energy consumption [9]. CE images are often blurred due to the complicated environment of the GI tract and inherent restrictions of the equipment in terms of image acquisition and transmission. Moreover, bad imaging conditions, such as low illumination in the GI tract will further degrade the quality of CE images. Finally, the short-focal-length image camera can only view a limited distance, which means the effects of depth are not ideal [24]. Figure 3.1 represents a few samples of noisy CE images.

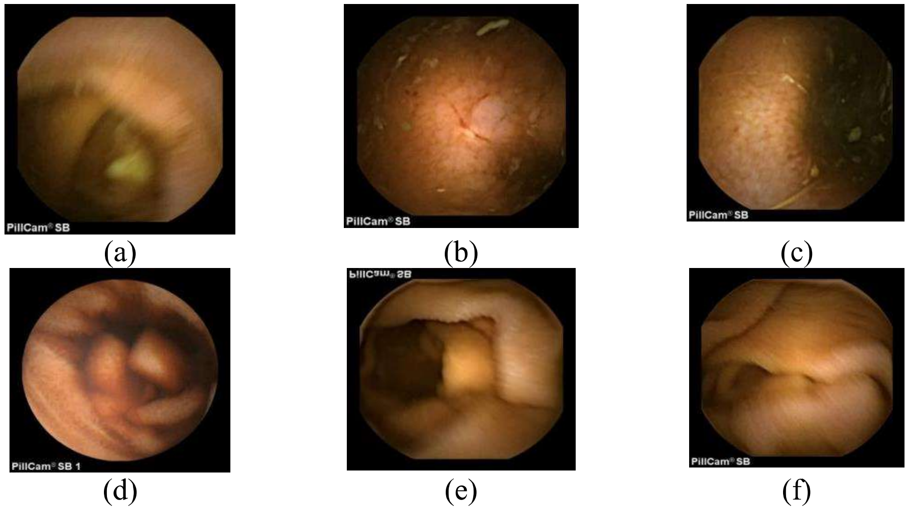

Figure 3.1: Sample of noisy CE images from (a) to (f)

Under these conditions, CE images exhibit Gaussian noise, motion blur, and poor contrast. Thus there is a need for a mechanism for restoration and enhancement of CE images. Image enhancement is the procedure to make a digital image more suitable for further analysis. Image restoration is an algorithmic procedure for restoring digital images degraded by noise contamination or blurring, or both [88]. Oblivious to image enhancement, image restoration is degradation modeling. It primarily removes the effects of degradation. The objective is to restore a degraded image to its original form as far as possible. Measurement of the degradation poses the challenge. If the complete analysis of degradation is known, then a simple inverse filtering process will solve the problem but, the correct estimation of degradation function is the problem. The estimation of degradation function is performed by observation, experimentation, and modeling.

The general form of a noisy image is defined by equation (3.1).

$$u_0(x, y) = u(x, y) + \eta(x, y) \tag{3.1}$$

where, $u_0(x, y)$ is the intensity function denoting pixel values of a noisy image, $u(x, y)$ is the desired clean image and η, is the noise. The measurement of quality of the image is obtained by Mean squared error (MSE), Peak Signal to noise ratio (PSNR), structural similarity (SSIM) index, mean structural similarity (MSSIM) index, edge strength similarity (ESSIM), signal-to-noise ratio (SNR) and contrast-to-noise ratio (CNR). Table 3.1 summarizes a few contributions towards the restoration and enhancement of CE images.

Table 3.1: Summary of the prior art

Prior Art	Approach	Results	Limitations
[24]	The adaptive contrast diffusion method	Accuracy=71.5% Sensitivity=69.5% Specificity=73.5%	More suitable convergence criteria required to make the process automatic and more reliable
[89]	Contrast-Limited Adaptive Histogram Equalization (CLAHE)	SSIM=0.79, PSNR=35.3, ESSIM=0.9	Removes random noise only
[88]	Total variation (TV) minimization	SNR=24.3148 dB	Generates stair case effect
[90]	Channel-by-channel (CBC) TV minimization and Color-TV (CTV) minimization	PSNR=31.5638 dB	Generates stair case effect
[91]	Improved Adaptive Gamma Correction Method (AGCM)	For AGCM (a=0.06) PSNR=6.38 dB CNR=7.48	Improves illumination but does not consider noise
[92]	Anisotropic Contrast Diffusion Enhancement Using Variance	-	Blurs important features such as edges
[93]	Discrete Cosine Transform (DCT) and Anisotropic Contrast Diffusion	Avg. PSNR =18.549 dB	Blurs important features such as edges

Following observations are derived from a detailed study of prior art and CE images:

a) CE images suffer from Gaussian noise
b) CE images suffer from motion blur
c) CE images pose a low contrast
d) Balanced smoothing is required to preserve both low frequency and high-frequency components

3.2 Methods and Model

Various techniques used for image restoration are inverse filtering, Wiener filtering, wavelet restoration and, blind deconvolution. Second and fourth-order partial differential equations (PDE) have proved to be a very useful image restoration tools. Based on the above-discussed problems and design criteria, this study proposes a novel framework for restoration and enhancement of capsule endoscopy images, as shown in Figure 3.2.

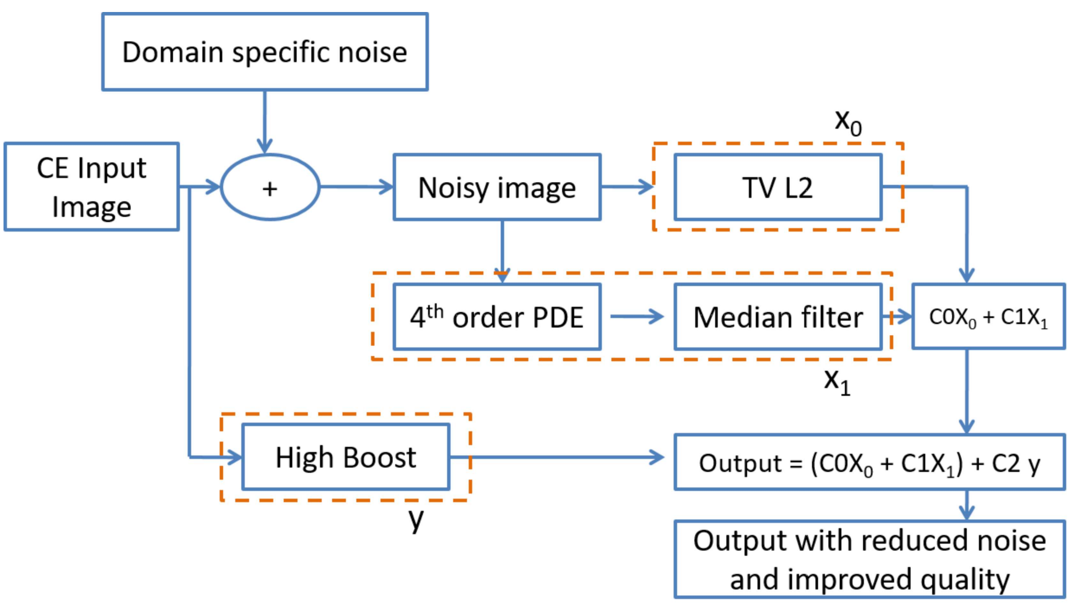

Figure 3.2: A framework for restoration and enhancement of capsule endoscopy images

A detailed explanation of proposed work as depicted in Figure 3.2 is given as below:

1. CE input image is normally degraded by Gaussian noise which is additive in nature.
2. CE input image is also subjected to motion blur.
3. Steps 1 and 2 produce the noisy and blurred images.
4. TV-L2 based method is applied to remove blur and avoids excessive smoothing however, it generates blocky artifacts. The component so obtained is termed as X_0.
5. Fourth-order PDE is capable of removing noise, preserve edges and avoid block artifacts but, it may tend to leave artifacts near edges.
6. To abolish the limitation, the Median filter is applied to the output of step 5 which removes the artifacts and enhances the image.
7. The combined result of steps 5 and 6 is termed as component X_1
8. To avoid excessive smoothing by both the noise removal components; X_0 and X_1 are added with the help of control parameter C0 and C1.
9. To restore the high-frequency components lost during the smoothing process high boost is applied and the resultant is termed as component Y
10. Finally, the output of the entire framework is given as $Output = (C0X_0 + C1X_1) + C2(Y)$.

Two control parameters $C0, C1$ and $C2$ regulate the blending of various components. The subsequent section discusses the detailed functioning of all the methods used in the proposed framework.

3.2.1 Total Variation (TV) Model

Amongst all the image restoration techniques, TV is the most suitable technique used for image de-noising. To recover de-noised image u from noisy image f over a 2D space, Rudin et. al [94] proposed the TV model. The main properties of the TV model are semi-continuity, convexity, and homogeneity due to which the problem of noise removal is converted to a minimization problem. It minimizes the following energy function:

$$\min_{u \epsilon BV(\Omega)} \|u\|_{TV(\Omega)} + \frac{\lambda}{2} \int_{\Omega} (f-u)^2 \, dx \tag{3.2}$$

where, $BV(\Omega)$ is the bounded variation over the domain Ω, $TV(\Omega)$ is the total variation over the domain, and λ is a penalty term. When u is smooth, the total variation is equivalent to the integral of the gradient magnitude given as:

$$\|u\|_{TV(\Omega)} = \int_{\Omega} \|\nabla_u\| \, dx \tag{3.2}$$

where $\|\cdot\|$ is the Euclidean norm. Then the objective function of the minimization problem becomes:

$$\min_{u \epsilon BV(\Omega)} \int_{\Omega} [\, \|\nabla_u\| + \frac{\lambda}{2}(f-u)^2 \,] dx \tag{3.3}$$

From this functional, the Euler-Lagrange equation for minimization – assuming no time-dependence – gives us the nonlinear elliptic partial differential equation:

$$\nabla \cdot \left(\frac{\nabla_u}{\|\nabla_u\|}\right) + \lambda \, (f-u) = 0 \, , u \, \epsilon \, \Omega \quad \text{while} \quad \frac{\partial \mathrm{u}}{\partial \mathrm{n}} = 0 \, , u \, \epsilon \, \partial\Omega \tag{3.4}$$

The time-dependent version the Euler-Lagrange equation for minimization is given as:

$$\frac{\partial \mathrm{u}}{\partial \mathrm{t}} = \nabla \cdot \left(\frac{\nabla_u}{\|\nabla_u\|}\right) + \lambda \, (f-u) \tag{3.5}$$

TV-L2 model can remove blur and preserve certain edge information. The L2 norm avoids excessive smoothing. The square terms blow up the error difference between outliers and minimization seeks to minimize data and outliers together.

3.2.2 Fourth Order Partial Differential Equations (PDE)

Second-order PDE includes TV minimization and anisotropic diffusion [95]. These techniques provide a smoothing by removing noise as well as preserving edge. However, in the pursuit of doing so, these techniques often tend to generate false edges or blocky effect. You et al. [95] proposed a class of fourth-order PDE, which tends to remove noise and preserve edge by minimizing a Laplacian of the image intensity function. The energy function is defined as follows:

$$E(u) = \int_{\Omega} f(|\nabla^2 \mathrm{u}|)d\Omega \tag{3.6}$$

where, u is the noisy image, Ω is the image domain, ∇^2 is the Laplacian operator, f is greater than zero and increasing function. Thus the minimization of functional given by equation (3.6) implies smoothing of the given image as measured by $|\nabla^2 \mathrm{u}|$. The equation (3.7) gives the corresponding Euler-Lagrange equation and equation (3.8) shows the marching of steepest descent.

$$\nabla^2 \left[f'(|\nabla^2 \mathrm{u}|) \frac{\nabla^2 \mathrm{u}}{|\nabla^2 \mathrm{u}|} \right] = 0 \tag{3.7}$$

$$\frac{\partial \mathrm{u}}{\partial \mathrm{t}} = -\nabla^2 \left[f'(|\nabla^2 \mathrm{u}|) \frac{\nabla^2 \mathrm{u}}{|\nabla^2 \mathrm{u}|} \right] \tag{3.8}$$

$$\frac{\partial \mathrm{u}}{\partial \mathrm{t}} = -\nabla^2 [c(|\nabla^2 \mathrm{u}|)\nabla \mathrm{u}] \tag{3.9}$$

The time evolution is stopped when an optimal solution with noise removal and edge preservation is reached. Thus, this stage can remove noise, preserve edges and avoid block effect but, it tends to leave artifacts near edges. These artifacts can be removed using simple filters such as a median filter. Median filter – a nonlinear filtering method, is very popular [96] and performs well for isolated noise. Its ability to preserve edge characteristics makes its performance satisfactory. Its working principle is to choose an intermediate value from a group of adjacent pixels ordered by their gray level [97]. Median filter reduces inhomogeneity [98].

3.2.3 High Boost to Retain the Lost Components

In CE images, there is a need to emphasize high-frequency components of the image details without removing the low-frequency components. Thus high boost filter is used to enhance high-frequency components while keeping the low-frequency components intact. The Laplacian operator used for high boost filtering highlights the gray-level discontinuities in an image and deemphasizes regions with slowly varying gray levels. It also generates a dark featureless background due to which adding the emphasized high-frequency components to the original image becomes very easy.

3.2.4 Control Parameters to Govern the Blending of the Model

The control parameters govern the proposed framework. C0 and C1 act as the control parameter to avoid excessive smoothing and excessive contrast while C2 acts as the enhancement factor. C0 and C1 control the blending of two intermediate output images generated by the TVL2 model and 4th order PDE. Their values are chosen experimentally. C2 controls the amount of high-frequency components added to the de-noised image. The values of both these parameters are chosen experimentally.

The final output so derived is given by equation (3.10).

$$Output = (C0X_0 + C1X_1) + C2(Y) \tag{3.10}$$

3.3 Results and Discussion

This section describes the dataset, performance metrics, and detailed result analysis. The overall performance of the proposed framework is shown with the help of statistical, graphical, and visual results.

3.3.1 Dataset and Experimental Setup

A total of 50 images of ulcer, bleeding, and normal cases from CE videos [9] are extracted. The dimension of each image is 576x576 pixels. The proposed framework is tested with these 50 images on various performance metrics and other approaches. The experiment is conducted on the Dell Optiplex 9010 machine with an Intel Core i7 processor and 6 GB RAM using MATLAB R2017a.

3.3.2 Performance Criteria

The performance of the proposed framework is measured based on MSE, SSIM, MSSIM, PSNR, and Entropy. The performance of the CAD system with and without the proposed restoration is measured based on accuracy, sensitivity, specificity, precision, f-measure and Matthews correlation coefficient (MCC) derived from the confusion matrix.

3.3.2.1 MSE measures the average of the squares of the errors between two quantities. The MSE is a measure of the quality of an estimator—it is always non-negative, and values closer to zero are better. For mxn image, MSE is computed by equation (3.11).

$$MSE = \frac{1}{mn}\sum_{x=1}^{m}\sum_{y=1}^{n}(f(x,y) - f'(x,y))^2 \tag{3.11}$$

Where, m and n are the dimensions of the image, $f(x,y)$ is the grayscale value of (x,y)th pixel in original image and $f'(x,y)$ is the grayscale value of the pixel in the de-noised image.

3.3.2.2 SSIM index [99] is based on similarities of local luminance, contrast, and structure between a reference image and a distorted image. Given two local image patches x and y, the local SSIM index is defined as

$$SSIM(x,y) = \frac{(2\mu_x\mu_y + c1)(2\sigma_{xy} + c2)}{(\mu_x^2 + \mu_y^2 + c1)(\sigma_x^2 + \sigma_y^2 + c2)} \tag{3.12}$$

where μ, σ, and σ_{xy} are the mean, standard deviation, and cross-correlation between the two patches, respectively. $c1$ and $c2$ are used to avoid instability when the means and variances are close to zero. SSIM compares local patterns of normalized pixel intensities [96]. SSIM index of the whole image is obtained by averaging the local SSIM indices calculated using a sliding window.

3.3.2.3 MSSIM: The overall image quality can be evaluated by Mean SSIM (MSSIM) [100], which is defined as

$$MSSIM(x,y) = \frac{1}{M}\sum\nolimits_{j=1}^{M} SSIM(x_j, y_j) \tag{3.13}$$

3.3.2.4 Entropy: Higher is the noise in the image; higher is the gray level distribution, leading to a higher value of entropy. Entropy is given by equation (3.14)

$$\text{Entropy} = \sum\nolimits_{i=1}^{G}(i * \log(p(i))) \tag{3.14}$$

where G is the number of gray levels, and $p(i)$ is the probability of occurrence of gray level i.

3.3.2.5 The Edge Preservation Index (EPI) [101] will calculate the amount of edges preserved in an image after de-noising.

$$EPI = \frac{\sum(\Delta I - \overline{\Delta I})(\Delta F - \overline{\Delta F})}{\sqrt{\sum(\Delta I - \overline{\Delta I})^2 (\Delta F - \overline{\Delta F})^2}} \tag{3.15}$$

where ΔI and ΔF are the high-pass filtered versions of images I and F and obtained with a 3×3 pixel standard approximation of the Laplacian operator. The larger value of EPI means more ability to preserve edges.

3.3.3 Results

The quantitative results of five different methods are evaluated upon the criterion mentioned in the preceding section. Table 3.2, Table 3.3, Table 3.4, Table 3.5 and Table 3.6 present a comparison between the proposed method with four other methods on the quantitative criterion of Entropy, MSE, PSNR, SSIM and MSSIM respectively. Similarly, Figure 3.3, Figure 3.4, Figure 3.5, Figure 3.6 and Figure 3.7 shows the graphical analysis of the results of Entropy, MSE, PSNR, SSIM and MSSIM respectively. Anupriya and Tayal [102] proposed a Self-Organizing Migration Algorithm (SOMA) for finding the optimal set of parameters for wavelet shrinkage denoising. In addition to SOMA, the proposed technique is compared with TV-L1[103], TV-L2 and fourth-order PDE [95] based image de-noising techniques. Figure 3.3 shows the graphical analysis of results.

Table 3.2 Performance comparison of Entropy at different variance level of noise

Method	Var=0.01	Var=0.025	Var=0.05	Var=0.075	Var=0.1
TV L1 [103]	6.745466	6.962762	6.814364	7.017663	7.04284
TV L2 [95]	6.90975	6.919409	6.933591	6.94976	6.950429
4th order PDE [95]	6.616575	6.867696	6.687202	6.92112	6.942583
SOMA [102]	6.695074	6.922337	6.76667	7.008143	7.020075
Proposed	5.910959	6.0255	5.9833	6.115719	5.8178

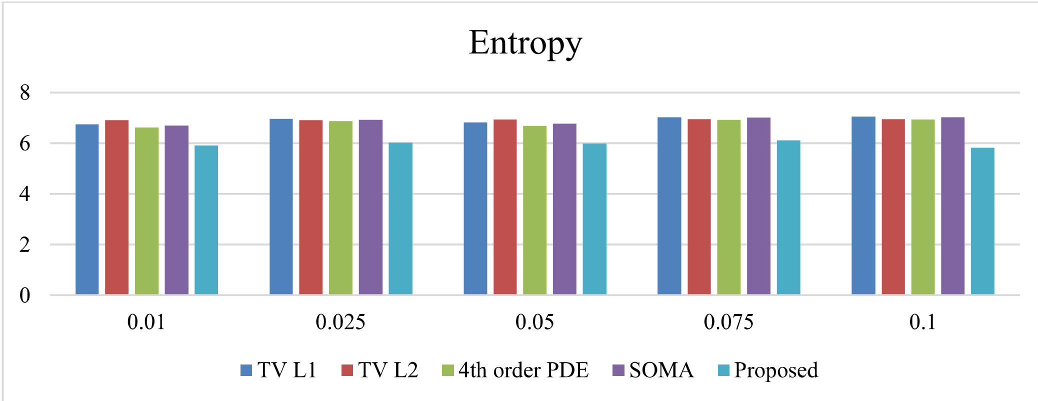

Figure 3.3: Graphical analysis of the result of Entropy

Table 3.3 Performance comparison of MSE at different variance level of noise

Method	Var=0.01	Var=0.025	Var=0.05	Var=0.075	Var=0.1
TV L1 [103]	0.00377845	0.004515602	0.006281633	0.009376991	0.013610707
TV L2 [95]	0.004996682	0.00509617	0.007044789	0.006257218	0.007686041
4th order PDE [95]	0.0037918	0.004557905	0.006298509	0.009410688	0.013657617
SOMA [102]	0.003662656	0.004393762	0.006175667	0.009379707	0.013533085
Proposed	0.0018	0.002429428	0.002223691	0.002429428	0.002429428

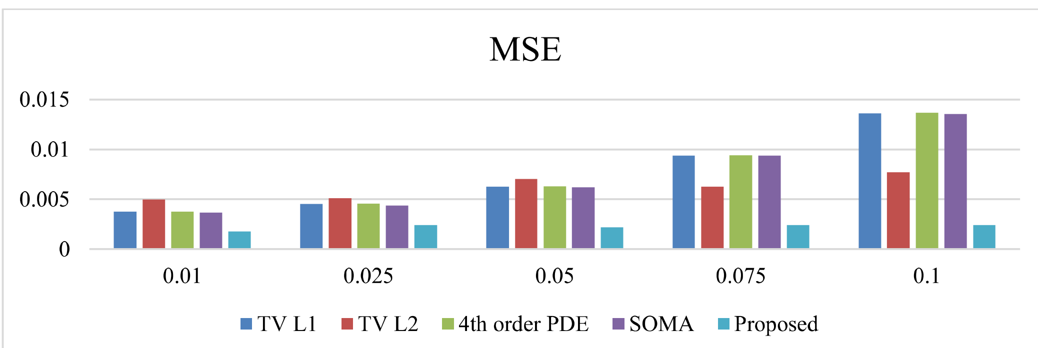

Figure 3.4: Graphical analysis of the result of MSE

Table 3.4 Performance comparison of PSNR at different variance level of noise

Method	Var=0.01	Var=0.025	Var=0.05	Var=0.075	Var=0.1
TV L1 [103]	72.41796346	71.61764233	70.19342304	68.44416451	66.82599258
TV L2 [95]	71.22996575	71.09236065	69.74552183	70.20098667	69.30777206
4th order PDE [95]	72.40589913	71.57714705	70.1828675	68.42858541	66.81105003
SOMA [102]	72.55328215	71.73643388	70.2669818	68.44290678	66.85083125
Proposed	74.74835619	74.30975877	74.3291	74.3308	74.30975877

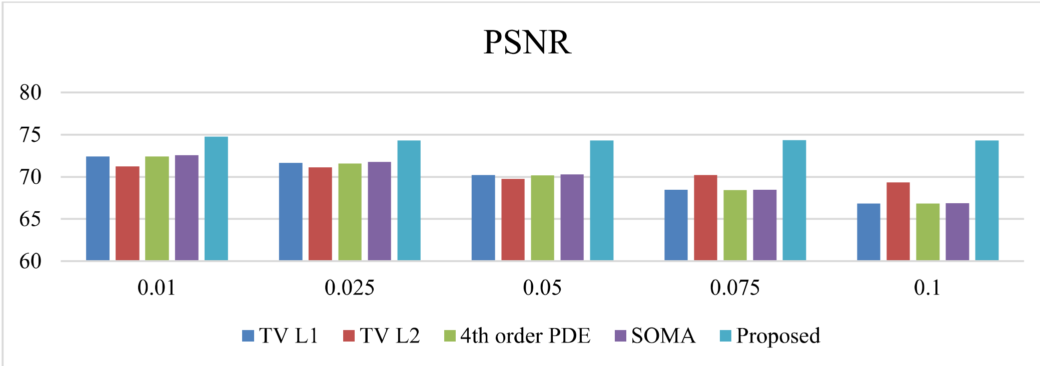

Figure 3.5: Graphical analysis of the result of PSNR

Table 3.5 Performance comparison of SSIM at different variance level of noise

Method	Var=0.01	Var=0.025	Var=0.05	Var=0.075	Var=0.1
TV L1 [103]	0.916896905	0.953245677	0.932248007	0.932822452	0.916896905
TV L2 [95]	0.918305759	0.932583221	0.922302336	0.926711042	0.918305759
4th order PDE [95]	0.916542475	0.95279407	0.932179866	0.932517507	0.916542475
SOMA [102]	0.918190008	0.954833247	0.934069306	0.93371122	0.918190008
Proposed	0.972	0.974010377	0.972057798	0.9661	0.974010377

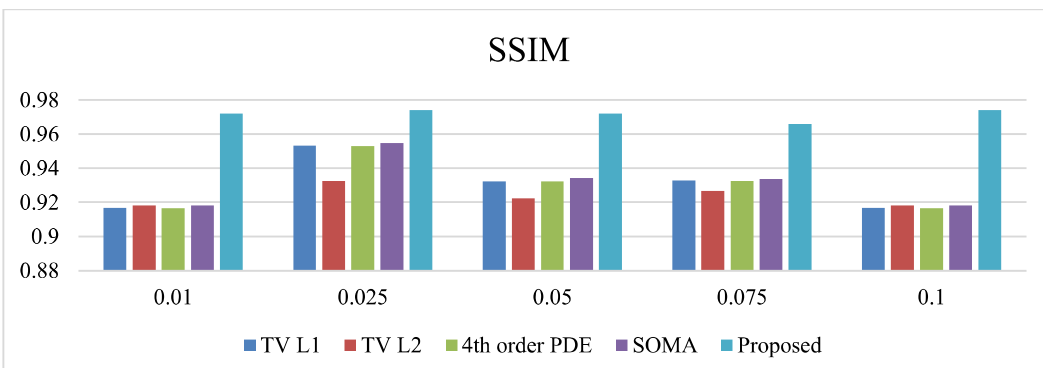

Figure 3.6: Graphical analysis of the result of SSIM

Table 3.6 Performance comparison of MSSIM at different variance level of noise

Method	Var=0.01	Var=0.025	Var=0.05	Var=0.075	Var=0.1
TV L1 [103]	0.602314984	0.613933915	0.584360078	0.594871098	0.584383738
TV L2 [95]	0.521147688	0.555921012	0.512708967	0.54747641	0.543303721
4th order PDE [95]	0.624698126	0.6359188	0.606708312	0.616204769	0.605968699
SOMA [102]	0.626313631	0.637547101	0.608232317	0.615772461	0.605361846
Proposed	0.9628	0.959197795	0.955412657	0.9457	0.9522

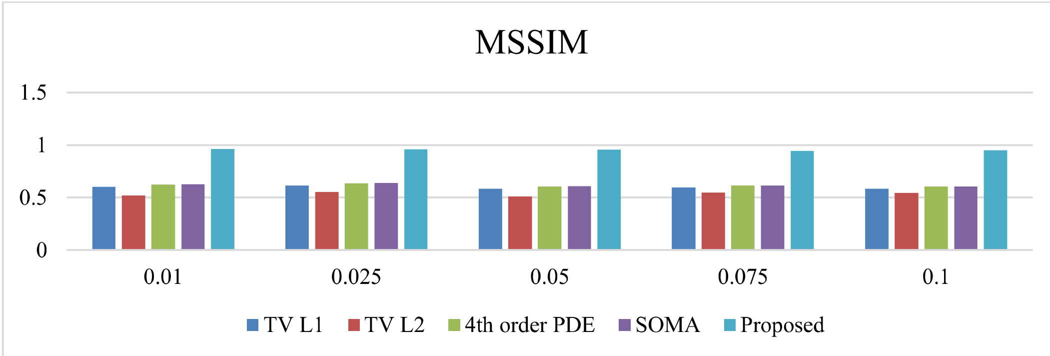

Figure 3.7: Graphical analysis of the result of MSSIM

Table 3.7 Performance comparison of EPI

Method	EPI
TV L1 [103]	0.2511
TV L2 [95]	0.1790
4th order PDE [95]	0.1403
SOMA [102]	0.6074
Proposed	0.6790

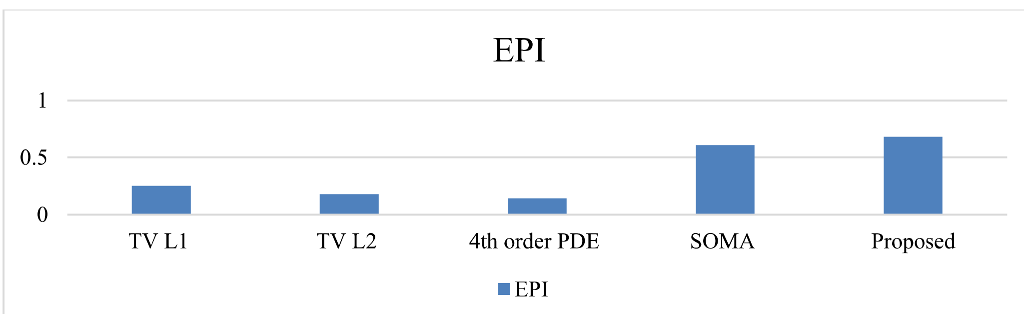

Figure 3.8: Graphical analysis of the result of EPI

As seen through the graphical analysis of the results, the proposed restoration framework performs better than other restoration methods under varied conditions. Also, the proposed method does not perform any trade-off towards computational time to achieve better performance.

Further, this study also analyzes the performance of the CAD system for GI tract abnormality detection in CE. Table 3.7 shows a comparative analysis of the CAD system with and without restoration on different performance criteria, and Figure 3.8 shows a graphical analysis of the same.

Table 3.8: Comparative analysis of CAD system with and without restoration

Approach	Accuracy	Sensitivity	Specificity	Precision	F-measure	MCC
Without restoration	0.83	0.83	0.94	0.83	0.83	0.77
With proposed restoration	0.85	0.85	0.95	0.86	0.85	0.80

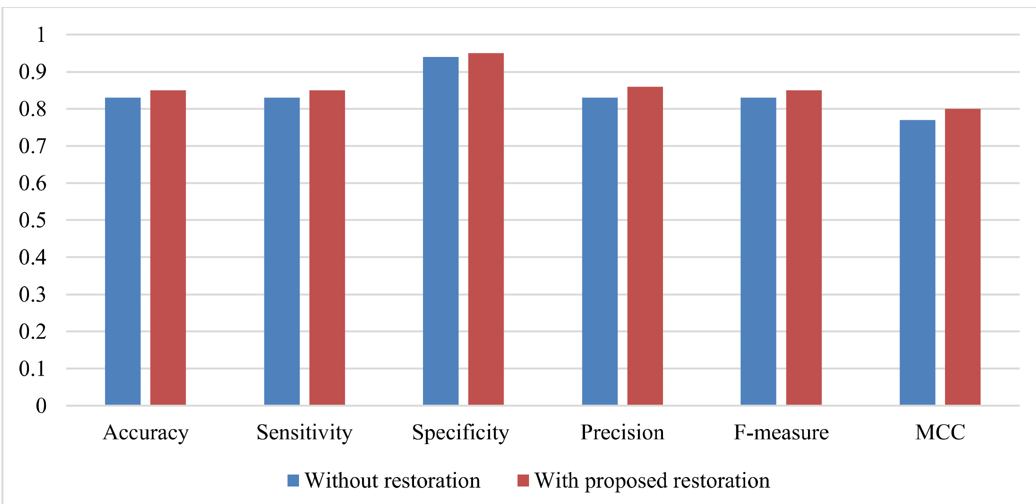

Figure 3.9: Graphical analysis of the performance of a CAD system

CAD system equipped with the proposed restoration method outperforms the CAD system without any restoration technique in all six performance criteria.

3.4 Conclusion

The proposed method outperforms four other state-of-the-art methods in all five performance criteria. The lower value of Entropy and MSE indicate better quality of the image while higher values of all other criteria, namely SSIM, MSSIM, and PSNR indicate a better quality image. The proposed approach is capable of noise removal while preserving a low level and a few high-level components leading to better results. Moreover, the CAD system for detecting an abnormality in the GI tract from CE images also performs better with the proposed restoration approach.